Journal of Hazardous Materials 184 (2010) 538–546

Contents lists available at ScienceDirect

Journal of Hazardous Materials

journal homepage: www.elsevier.com/locate/jhazmat

Rapid removal and recovery of Pb(II) from wastewater by magnetic nanoadsorbents

Nashaat N. Nassar*

Department of Chemical and Petroleum Engineering, University of Calgary, Calgary, Alberta, Canada

ARTICLE INFO

Article history:
Received 3 March 2010
Received in revised form 23 June 2010
Accepted 18 August 2010
Available online 26 August 2010

Keywords:
Lead
Nanoadsorbent
Iron oxide
Wastewater
Adsorption
Equilibrium
Nanoparticle

ABSTRACT

Iron oxide nanoadsorbents are cost-effective adsorbents that provide high adsorption capacity, rapid adsorption rate and simple separation and regeneration. In this study, Fe_3O_4 nanoadsorbents have been employed for the removal of Pb(II) ions from aqueous solutions by a batch-adsorption technique. The effects of contact time, initial concentration of Pb(II) ions, temperature, solution pH and coexisting ions on the amount of Pb(II) adsorbed have been investigated. Pb(II) adsorption was fast, and equilibrium was achieved within 30 min. The amount of Pb(II) adsorbed increased as temperature increased, suggesting an endothermic adsorption. The optimal pH value for Pb(II) adsorption was around 5.5. Furthermore, the addition of coexisting cations such as Ca^{2+}, Ni^{2+}, Co^{2+}, and Cd^{2+} has no remarkable influence on Pb(II) removal efficiency. The adsorption equilibrium data fitted very well to Langmuir and Freundlich adsorption isotherm models. The thermodynamics of Pb(II) adsorption onto the Fe_3O_4 nanoadsorbents indicated that the adsorption was spontaneous, endothermic and physical in nature. The desorption and regeneration studies have proven that Fe_3O_4 nanoadsorbents can be employed repeatedly without impacting its adsorption capacity.

1. Introduction

The presence of toxic metal ions in wastewater remains a serious environmental concern. Therefore, it is necessary to develop various efficient technologies for their removal. A number of techniques have been used to remove the metal ions from wastewater effluents; including chemical precipitation [1], ion exchange process [2,3], electrolytic methods [4], adsorption onto activated carbon [5], organic-based ligand precipitation [6], membrane and reverse osmosis processes [7]. These methods have been found to be limited, because of the high capital and operating costs and/or the ineffectiveness in meeting stringent effluent standards. Therefore, several approaches have been studied for the development of inexpensive and abundant metal sorbents, such as sawdust [8], live biomass [9], clay [10,11] and agricultural byproducts [12–14]. These approaches, however, suffer from some challenges; including the huge amount of sludge waste generated from the spent adsorbents, the high regeneration cost and the low adsorption rate and capacity, especially at very low pollutant concentration [15,16]. An excellent adsorbent should generally possess high surface area and short adsorption equilibrium time, so that it can be used to remove high amount of pollutant in shorter time. In addition, it should generate a minimum amount of sludge. Nanoadsorbents could be employed most effectively not only in a very low concentration range (~1 ppm) of pollutant, but also in a very high concentration range (~1000 ppm), where other techniques are ineffective, time-consuming, or costly. Nanoadsorbents have particularly high adsorption capacities because of their specific functionality and large specific surface areas, i.e., surface area per unit mass. In addition, nanoadsorbents are highly mobile in porous media because they are much smaller than the relevant pore spaces, so they can be transported effectively by the flow in porous media [17]. Therefore, the nanoadsorbents can be employed *in situ*, within the contaminated zone where treatment is needed. *In situ*, involves treatment of contaminants in place, in comparison to ex situ where treatment occur after transferring the contaminated material to a more convenient location [17], adding more cost and environmental impact to the process (e.g. pumping, transportation, instrumentations and treatment of contaminants). Certain types of nanoadsorbents have been found to be effective in metal ion removal [15,18–21]. Although previous research has highlighted the ability of metal oxide nanoadsorbents for metal ion adsorption, few metal ions were actually tested [15,20–23]. Furthermore, the reported literature looked into percentage removal without deep investigation onto the adsorption mechanism and thermodynamic parameters. In the present study, the adsorption mechanistic, kinetics, equilibria and thermodynamic of Pb(II) ions, as an example of a typical heavy metal ion present in wastewater, onto the Fe_3O_4

* Corresponding author. Tel.: +1 403 210 9772; fax: +1 403 210 3973.
E-mail address: nassar@ucalgary.ca.

0304-3894/$ – see front matter © 2010 Elsevier B.V. All rights reserved.
doi:10.1016/j.jhazmat.2010.08.069

Nomenclature

C	concentration of Pb(II) in the solution at any time (mg/L)
C_{ads}	amount of Pb(II) adsorbed onto the nanoadsorbents (mg/L)
C_{des}	amount of Pb(II) released into the aqueous solution (mg/L)
C_e	equilibrium concentration of Pb(II) in the solution (mg/L)
C_o	initial concentration of Pb(II) in the solution (mg/L)
K	adsorption equilibrium constant (dimensionless)
K_F	Freundlich isotherm constant (mmol/g)(L/mmol)$^{1/n}$
K_L	Langmuir isotherm constant (L/mmol)
m	mass of Fe_3O_4 nanoparticles (g)
q	amount of Pb(II) adsorbed at any time (mg/g)
q_e	amount of Pb(II) adsorbed at equilibrium time (mg/g)
q_m	maximum equilibrium adsorption capacity of Pb(II) (mg/g)
r	(%) recovery efficiency of Pb(II)
R	ideal gas constant (R = 8.314 J/mol K)
V	total volume of aqueous solution (L)
$1/n$	Freundlich heterogeneity factor (unitless)
ΔG^o_{ads}	standard Gibbs free energy change (kJ/mol)
ΔH^o_{ads}	standard enthalpy change (kJ/mol)
ΔS^o_{ads}	standard entropy change (J/mol K)

Subscripts

ads	adsorption
des	desorption
e	equilibrium
o	initial
m	maximum
F	Freundlich
L	Langmuir
zpc	zeropoint of charge

nanoadsorbents were investigated. In addition, the effect of solution pH, coexisting cations, and initial Pb(II) concentration on the adsorption was studied. Furthermore, the Langmuir and Freundlich models were used to describe the equilibrium isotherms.

2. Experimental

2.1. Adsorbent

Fe_3O_4 nanoparticles obtained from Nanostructured & Amorphous Materials, Inc., Houston, TX, were used as nanoadsorbents. Before any adsorption experiments were conducted, the characteristics of the selected nanoadsorbents were evaluated; namely: particle size, structure, specific surface area (BET), pore volume and external surface area. Results are presented in Table 1. The surface areas and pore volume of the nanoadsorbents were measured by performing N_2-adsorption and desorption at 77 K, using a surface area and porosity analyzer (TriStar II 3020, Micromeritics Corporate, Norcross, GA). The samples were degassed at 423 K under N_2 flow overnight before analysis. Surface area was calculated using Brunauer-Emmet-Teller (BET) equation. External surface areas were obtained by t-plot method and there was no significant difference between the surface areas obtained by BET and t-plot methods. This indicates that the nanoadsorbents have no significant porosity and maintain a high external surface area. Structure and particle size were determined by using X-ray Ultima III Multi Purpose Diffraction System (Rigaku Corp., The Woodlands, TX) with Cu KR radiation operating at 40 kV and 44 mA with a θ–2θ goniometer. Scanning was performed from 8° to 90° with a counting time of 0.2 s/step. The structure was identified by comparison to spectra in the JADE program, Materials Data XRD Pattern Processing Identification & Quantification. The diffraction pattern is shown in Fig. 1. Clearly, it conforms the peaks of Fe_3O_4 as reported by the manufacturer. Measurements on particle size indicated that the Fe_3O_4 nanoadsorbents have a size of 22 ± 1.5 nm.

Separation of nanoadsorbents from aqueous solution was evaluated by separating them via a small horseshoe Alnico magnet. The concentrations of the nanoadsorbents in the supernatant were evaluated at different pH values between 2.5 and 6.5 using the inductively coupled plasma-atomic emission spectroscopy (ICP-AES) (IRIS Intrepid II XDL, Thermo-Instruments Canada Inc., Mississauga, ON). No significant Fe concentrations were detected as confirmed by the ICP, indicating that all the nanoadsorbents were separated by the magnet and the dissolution of the nanoadsorbents under the considered experimental conditions was insignificant.

2.2. Adsorbates

$Pb(NO_3)_2$ obtained from ACROS Organics (99%, ACROS Organics, NJ) was selected for this study as a source of Pb(II) ions. Pb(II) stock solution was prepared by dissolving a specified weight of $Pb(NO_3)_2$ in 500 mL of deionized water, and subsequently diluted to the required concentrations. The following chemicals were used as the precursor salts for the coexisting cations present in wastewater, namely $Ni(NO_3)_2{\cdot}6H_2O$ (99.9985%, Alfa Aesar, Toronto, ON), $Cd(NO_3)_2{\cdot}4H_2O$ (99%, Fisher Scientific, Toronto, ON), $Ca(NO_3)_2{\cdot}4H_2O$ (99.9%, Fisher Scientific, Toronto, ON) and $Co(NO_3)_2{\cdot}6H_2O$ (99%, Fisher Scientific, Toronto, ON). All chemicals were used without further purifications.

2.3. pH measurements

pH measurements were performed with a AB15 plus pH meter from Fisher Scientific, Toronto, ON. Aliquots of 0.1 M HNO_3 or 0.1 M NaOH were used to adjust the pH over the range 2.5–6.5. In adjusting the pH, care was taken not to change significantly the initial concentration of Pb(II) ions in solution. Therefore, different NaOH and HNO_3 solution of optimum concentration were used to achieve the desired pH values mentioned above and the added volume of acid or base solution was kept $\leq$50 μL.

2.4. Adsorption of Pb(II) ions onto Fe_3O_4 nanoadsorbents

Batch-adsorption studies were performed by mixing nanoadsorbents with Pb(II) aqueous solution at a ratio 10:1 (g/L, mass of nanoadsorbents/volume of solution). Kinetics and equilibrium adsorption of Pb(II) ions onto the nanoadsorbents were carried out at different temperatures, namely 298, 313 and 328 K. 100 mg dry powder of nanoadsorbents was introduced into a 20-mL vial directly. Then 10 mL of Pb(II) aqueous solution with known initial concentration, C_o (mg/L), ranging from 10 to 800 mg/L was added to each vial. The vials were sealed and were shaken at 200 rpm in a temperature incubator at a pre-selected temperature for a required specific time. The Pb(II)-nanoadsorbents were separated from the mixture by a small horseshoe Alnico magnet, and the supernatant was decanted. The concentration of Pb(II) in the supernatant was measured by using inductively coupled plasma-atomic emission spectroscopy (ICP-AES). Pb(II) stock standard was prepared by dissolving a specified mass of the corresponding $Pb(NO_3)_2$ in deionized water. Standards containing 0.1, 1 and 10 ppm were prepared by diluting 50 ppm of the stock standard in deionized water. Accordingly, a four-point calibration curve was constructed.

Table 1
Characterizations of Fe_3O_4 nanoadsorbents considered in this study.

Manufacturer reported surface area (m^2/g)	Manufacturer reported particle size (nm)	X-ray measured particle size (nm)	Estimated BET surface area (m^2/g)	External surface area (m^2/g)	Average Pore volume (cm^3/g)
40	20–30	22 ± 1.5	43	39	0.38

A typical standard error in the metal concentration measurements was ±0.001 ppm. The equilibrium adsorption capacity, Q_e, of Pb(II) aqueous was calculated using the mass balance, according to the following equation [3]:

$$Q_e = \frac{C_o - C_e}{m} V \quad (1)$$

where V is the sample volume (L), m is the mass of Fe_3O_4 nanoadsorbents (g), C_o is the initial concentration of Pb(II) in the solution (mg/L), and C_e is the equilibrium concentration of Pb(II) in the solution (mg/L). For time-dependent data, C replaces C_e and Q replaces Q_e in Eq. (1).

2.5. Effect of coexisting cations

Multi-metal cation adsorption of nanoadsorbents was examined in the presence of the following coexisting cations Pb^{2+}, Ca^{2+}, Ni^{2+}, Co^{2+}, and Cd^{2+}. A sample containing a mixture of Pb^{2+} with the aforementioned cations was prepared at pH of 5.5 and 298 K. Concentration of each cation was maintained at approximately 100 mg/L.

2.6. Desorption of Pb(II)

In this experiment, desorption of Pb(II) from Pb-loaded nanoadsorbents was performed using HNO_3 solution at different concentrations. Nanoadsorbents containing Pb(II) was exposed to 10 mL solution of different HNO_3 concentrations, namely 0, 1, 5 and 10 mM. The mixture was agitated at 200 rpm and 298 K in a temperature incubator for 2 h. After desorption, the nanoadsorbents were separated by a small horseshoe Alnico magnet, and the supernatant was decanted for Pb(II) concentration measurement. The recovery efficiency, r (%), of Pb(II) from the solid phase was calculated as follows:

$$r(\%) = \frac{C_{des}}{C_{ads}} \times 100 \quad (2)$$

where C_{des} and C_{ads} are the amount of Pb(II) released into the aqueous solution and the amount of Pb(II) adsorbed onto the Fe_3O_4 nanoadsorbents (mg/L), respectively.

2.7. Reusability of nanoadsorbents

To test the reusability of the nanoadsorbents, the Fe_3O_4 nanoadsorbents containing Pb(II) were washed with HNO_3 solution of pH values between 2 and 3 until no detectable Pb(II) was observed in the wash water, as confirmed by the ICP. After that, Fe_3O_4 nanoadsorbents were thoroughly washed with deionized water till the pH of the wash water reached the range of 5.0–6.5. Then, the washed nanoadsorbents were vacuum dried at 60 °C for 24 h and re-used for the subsequent adsorption cycle. Five cycles of consecutive adsorption–desorption–regeneration were carried out to validate the reusability of Fe_3O_4 nanoadsorbents for the removal and recovery of Pb(II).

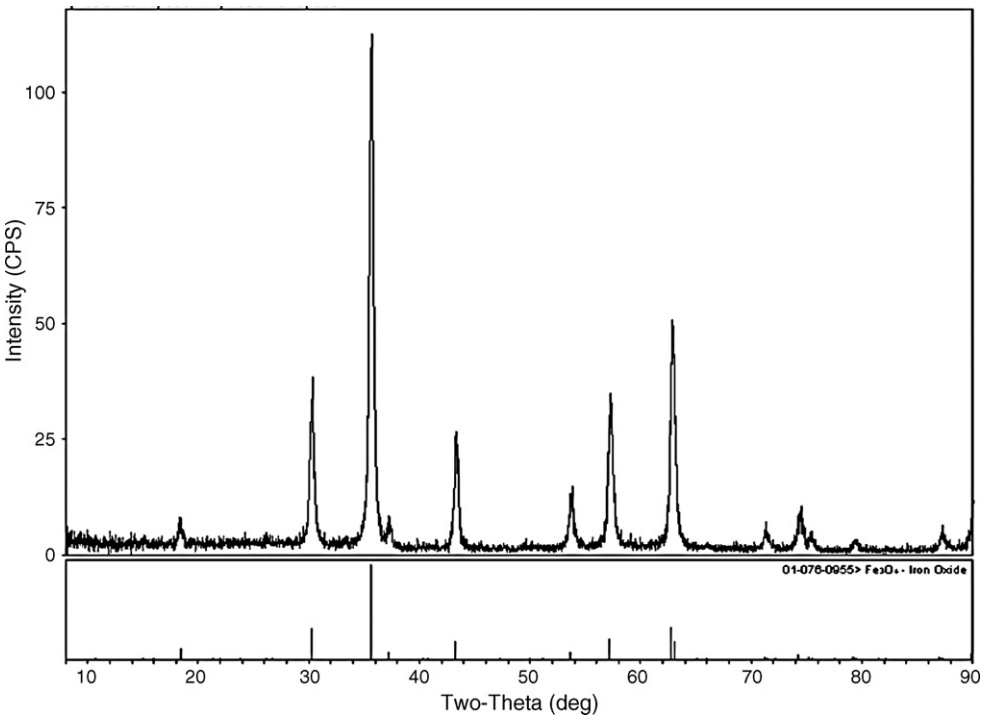

Fig. 1. X-ray diffractograms of selected nanoadsorbents. Reference data for Fe_3O_4 are from Materials Data XRD Pattern Processing Identification & Quantification.

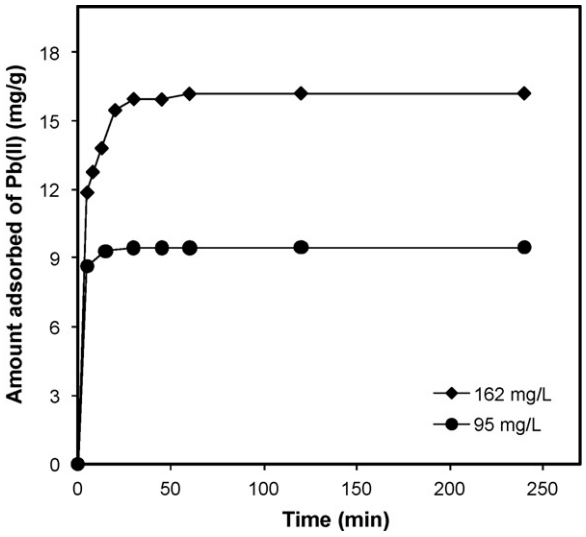

Fig. 2. Effect of contact time on the removal of Pb(II) at different initial concentrations. Adsorbent dose: 10 g/L, shaking rate: 200 rpm, pH: 5.5, *T*: 298 K.

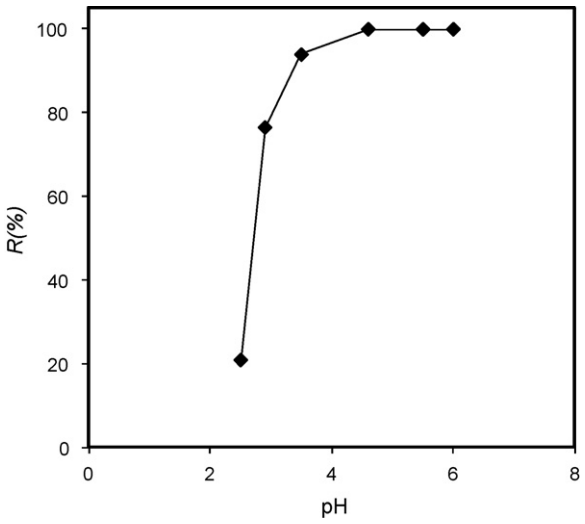

Fig. 3. Effect of pH on Pb(II) adsorption onto Fe_3O_4 nanoadsorbents. Initial Pb(II) concentration: 220 mg/L, adsorbent dose: 10 g/L, shaking rate: 200 rpm, contact time: 24 h, *T* = 298 K.

3. Results and discussions

3.1. Adsorption mechanism

In aqueous solution, the Pb(II) ions undergo solvation and hydrolysis as per the following reactions [24,25]:

$$Pb^{2+} + nH_2O \leftrightarrow Pb(H_2O)_n^{2+} \quad (R1)$$

$$Pb(H_2O)_n^{2+} \leftrightarrow Pb(H_2O)^{n-1} + H^+ \quad (R2)$$

$$Pb^{2+} + mH_2O \leftrightarrow Pb(OH)_m^{(2n-m)} + mH^+ \quad (R3)$$

Literature on Pb(II) speciation shows that the dominant species is $Pb(OH)_2$ at pH > 6.5 and Pb^{2+} and $Pb(OH)^+$ at pH < 6.5 [24]. In the meantime, the surface of metal oxide nanoadsorbents may undergo protonation/deprotonation as per reaction (R4) [26,27].

$$H_2O + M\text{–}O^- \underset{OH^-}{\overset{H^+}{\longleftrightarrow}} M\text{–}OH \underset{OH^-}{\overset{H^+}{\longleftrightarrow}} M\text{–}OH_2^+ \quad (R4)$$

where H^+ and OH^- refer to the potential determining ions.

The adsorption process is likely to be electrostatic attraction. In the basic solution, a significantly high electrostatic attraction exists between the negatively charged surface of the adsorbent and the Pb(II). As the pH of the solution decreases, the number of positively charged sites increases and the number of negatively charged sites decreases. A positively charged surface site on the nanoadsorbent does not favor the adsorption of Pb(II) ions, due to the electrostatic repulsion. In addition, in an acidic environment, at low pH values, excess hydrogen ions compete with the Pb(II) ions for the adsorption site resulting in lower adsorption of Pb(II).

3.2. Effect of contact time and initial Pb(II) concentration

The adsorption of Pb(II) onto nanoadsorbents was monitored for 250 min. The initial Pb(II) concentrations were 95 and 162 mg/L, respectively, the initial pH value of solution was 5.5, and the solution temperature was 298 K. As seen in Fig. 2, Pb(II) was adsorbed onto Fe_3O_4 nanoadsorbents quickly, and equilibrium was achieved within 30 min, independent of the initial concentration of Pb(II). This could be due to the small size of Fe_3O_4 nanoadsorbents, which was favorable for the diffusion of Pb(II) ions from bulk solution onto the active sites of the solid surface. Apparently, external adsorption dominated and no pore diffusion was observed to slow down the adsorption rate. Despite the short equilibrium time a 24-h contact time was adopted for the subsequent experiment to ensure attaining adsorption equilibrium. The short equilibrium time is in agreement with that reported by other researchers for the adsorption of other metal ions onto iron oxide nanoparticles [23,28,29]. In different to other conventional porous adsorbents in which adsorption occur through pore diffusion steps, which in turn slows down the adsorption rate [3]. Fe_3O_4 nanoadsorbent is a nonporous adsorbent, as confirmed by surface area and porosity measurement, where only external adsorption occurs. This type of adsorption mass transfer requires less time to reach equilibrium [30]. This result is promising as equilibrium time plays a major role in wastewater treatment plant economic viability. Also, as seen in Fig. 2, the amount adsorbed of Pb(II) increased with the increase in the initial concentration of Pb(II) in solution. This can be attributed to the increase in the ion occupancy number which favored the adsorption process.

3.3. Effect of pH

It is well known that pH is one of the most important factors which affect the adsorption process. Experiments were performed to find the optimum pH on the adsorption of Pb(II) ions onto Fe_3O_4 nanoadsorbents using different initial pH values changing from 2.5 to 6.5. A pH value of 6.5 was not exceeded, since increasing pH to 7.0, at fixed values of other variables, resulted in the precipitation of lead hydroxide [24]. Therefore, it was not possible to carry out adsorption experiments for Pb(II) at pH > 6.5. This would introduce uncertainty into the results.

Fig. 3 presents the effects of pH on the adsorption of Pb(II). As seen, the removal of Pb(II) ions is clearly pH dependent with the highest adsorption occurring at pH ≥ 5.5. Such pH effect has been observed for the adsorption of Pb(II) onto bulk iron oxides [31]. Higher pH is favorable for the deprotonation of sorbent surface [26,27]. Increased deprotonation results in the increase of the negatively charged sites, which enhances attractive forces between the sorbent surface and the Pb(II) ions, and thus results in an increase in the adsorption capacity. In the lower pH region, on the other hand, the positively charged sites dominate, this enhances the repulsion forces existing between the sorbent surface and the Pb(II) ions, and therefore decreases the adsorption of Pb(II) ions.

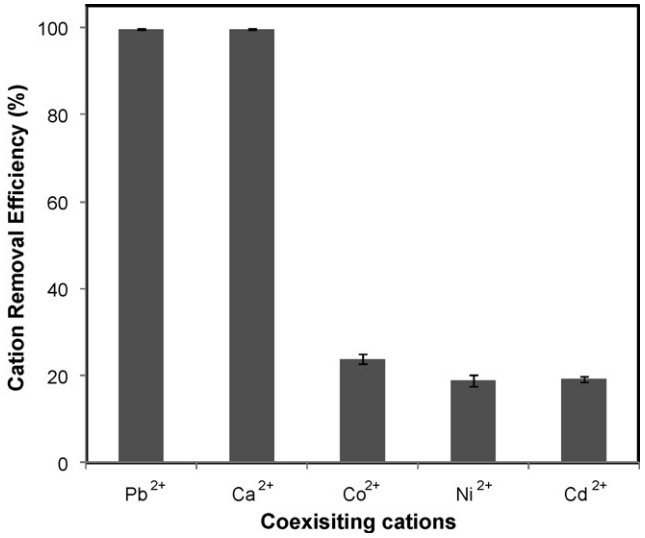

Fig. 4. Effect of coexisting ions on Pb(II) removal. Initial cation concentration: 100 mg/L, adsorbent dose: 10 g/L, shaking rate: 200 rpm, contact time: 24 h, pH 5.5, T = 298 K.

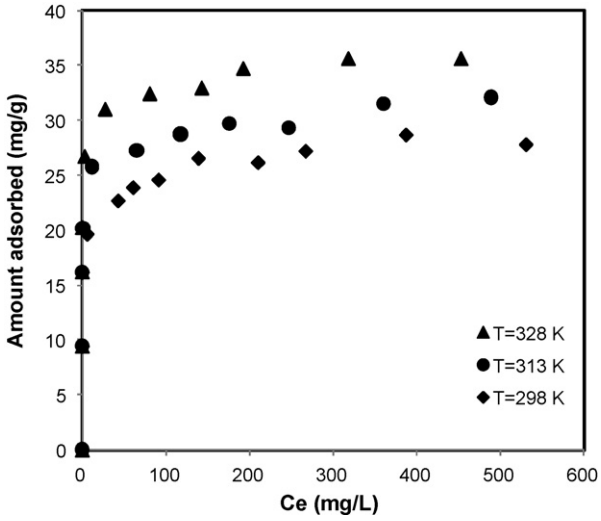

Fig. 5. Effect of temperature on the adsorption of Pb(II). Adsorbent dose: 10 g/L, shaking rate: 200 rpm, contact time: 24 h, pH 5.5.

3.4. Effect of coexisting cations

Generally, wastewater contains more than one cation. Thus, the presence of other cations may interfere in the removal efficiency of Pb^{2+}. As a result, the effects of the following coexisting cations on the Pb^{2+} adsorption were studied, namely Ca^{2+}, Ni^{2+}, Co^{2+}, and Cd^{2+}. The results are shown in Fig. 4. Results are the means of triplicate runs performed on different days with freshly prepared samples.

Surprisingly, the presence of these coexisting cations has no remarkable influence on Pb(II) removal efficiency. In addition, Ca^{2+} ions and some of the Ni^{2+}, Co^{2+}, and Cd^{2+} ions were able to adsorb onto the nanoadsorbents. In general, the competitive adsorption ability varies from one metal ion to another and is related to a number of factors, such as molecular mass, ion charges, hydrated ionic radius and hydration energy of the metals [32]. Apparently, the coexisting cations did not compete with Pb(II) ions for the active sites on the nanoadsorbents, suggesting a multi surface adsorption [33].

3.5. Effect of temperature

Temperature plays key roles on the adsorption process [35]. First, increasing the temperature decreases the viscosity of the solution which, in turn, enhances the rate of diffusion of the adsorbate molecules across the external boundary layer of the adsorbent and resulted in higher adsorption. Second, changing the temperature may affect the equilibrium adsorption capacity of the adsorbent. For instance, the adsorption capacity will decrease upon increasing the temperature for an exothermic reaction; while it will increase for an endothermic one. Hence, a study of the temperature-dependent adsorption processes provides valuable information about the standard Gibbs free energy, enthalpy and entropy changes accompanying adsorption. In this study, a series of experiments were conducted at 298, 313 and 328 K to investigate the effect of temperature on Pb(II) adsorption and determine the adsorption isotherms and thermodynamic parameters. Fig. 5 shows the amount of Pb(II) adsorbed onto Fe_3O_4 nanoadsorbents at different temperatures. As seen in the figure, the amount of Pb(II) adsorbed increases as the temperature increased. This increase suggests that the adsorption process is an endothermic one. The increase in the Pb(II) adsorption with temperature may be due the increase in ions mobility, which in turn increases the number of ions that interacted with active sites at the adsorbent surfaces. Similar observations have been reported by other researchers for the adsorption of Pb(II) onto metal oxide surfaces [36,37].

3.6. Adsorption isotherms

One of the most important characteristics of an adsorbent is the amount of adsorbate it can accumulate, which is calculated from the adsorption isotherms. Adsorption isotherms are constant–temperature equilibrium relationship between the amount of adsorbate per unit of adsorbent (Q_e) and its equilibrium solution concentration (C_e). A number of mathematical models have been employed for describing this equilibrium relationship. Out of several models, Freundlich and Langmuir models have been reported most frequently [38,39]. Eqs. (3) and (4) represent the Freundlich and the Langmuir models, respectively. The linear forms of the Freundlich and the Langmuir models are given by Eqs. (5) and (6), respectively.

$$Q_e = K_F C_e^{1/n} \tag{3}$$

$$Q_e = Q_m \frac{K_F C_e}{1 + K_L C_e} \tag{4}$$

$$\log Q_e = \log K_F + \frac{1}{n} \log C_e \tag{5}$$

$$\frac{C_e}{Q_e} = \frac{1}{Q_m K_L} + \frac{C_e}{Q_m} \tag{6}$$

where Q_e is the amount of Pb(II) adsorbed onto the nanoadsorbents (mmol/g), C_e is the equilibrium concentration of Pb(II) in supernatant (mM), K_F and n are Freundlich constants. K_F is roughly an indicator of the adsorption capacity ((mmol/g) (L/mmol)$^{1/n}$), and $1/n$ is the adsorption intensity factor (unitless). Specifically, a larger K_F value suggests a greater adsorption capacity, and a lower $1/n$ value indicates stronger adsorption strength. K_L is the equilibrium Langmuir adsorption constant related to the affinity of binding sites (L/mmol). Q_m (mmol/g) is the saturation capacity, representing the maximum amount of the Pb(II) adsorbed per unit weight of nanoadsorbents for complete monolayer coverage. The adsorption isotherms were determined using batch tests at different temperatures (Fig. 5) and pH = 5.5. Initial Pb(II) concentration was varied from 0 to 800 mg/L.

As seen in Fig. 5, Pb(II) adsorption increased sharply at low equilibrium concentration and starts to level off, suggesting that Fe_3O_4

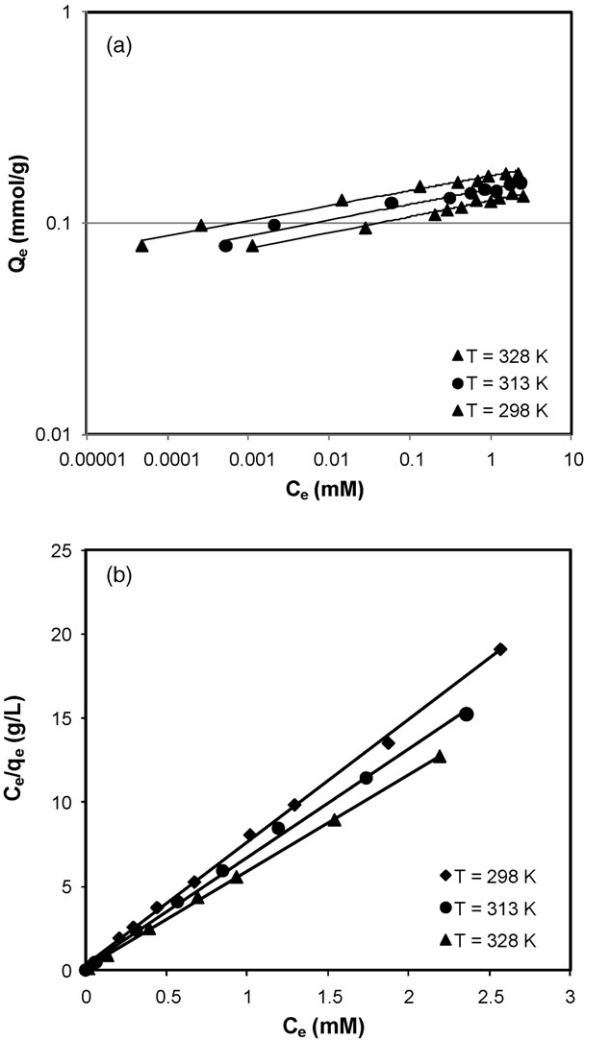

Fig. 6. Freundlich and Langmuir isotherms of Pb(II) onto Fe_3O_4 nanoadsorbents at different temperatures. Adsorbent dose: 10 g/L, shaking rate: 200 rpm, contact time: 24 h, pH 5.5.

has a high sorption affinity for Pb(II) even at low concentration. In addition, an increase in the solution temperature favors the Pb(II) adsorption as explained earlier. The Freundlich and Langmuir linear plots are presented in Fig. 6a and b. The adsorption data in Fig. 6a and b were fitted very well for both Freundlich and Langmuir models with correlation coefficients $R^2 \sim 0.99$. Nonetheless, for comparing the best fitting of Freundlich and Langmuir models non-linear Chi-square analysis [40] were conducted as per Eq. (7)

$$\chi^2 = \sum \frac{(Q_e - Q_{e\,Model})^2}{Q_{e\,Model}} \quad (7)$$

where Q_e and $Q_{e\,Model}$ are the equilibrium adsorption capacity obtained experimentally and modeling, respectively. If the model is in well agreement with the experimental data the χ^2 value would be small, the smaller χ^2 value the better agreement is with the model. The adsorption constants obtained from the isotherms together with χ^2values are listed in Table 2. Clearly, Freundlich model seems to be the best-fitting model for the experimental data. It is noteworthy that Langmuir model assumes that adsorption occurs on a homogeneous surface; while Freundlich model describes adsorption where the adsorbent has a heterogeneous surface with adsorption sites that have different adsorption energies. The values of $(1/n)$ in Table 2 indicate that n values are greater than unity suggesting that Pb(II) ions are favorably adsorbed by the nanoadsorbents. Furthermore, K_F values increased as the temperature increased suggesting an increase in the adsorption capacity with temperature as was confirmed experimentally. A comparison of the maximum uptake of Pb(II) ions onto different adsorbents is given in Table 3. As seen, the maximum uptake of Pb(II) ions onto Fe_3O_4 nanoadsorbents was approximately 1–35 times higher than that of reported low cost adsorbents [11,37,41–50]. This may be attributed to effect of particle size and distribution, surface area, morphology, surface structure and properties. However, higher adsorption capacities of Pb(II) have been reported by other researchers [24,51–53]. Nonetheless, this comparison is not precise, since the experimental conditions are different.

Table 3
Maximum adsorption capacity of Pb(II) ions onto various adsorbents.

Adsorbent	Maximum adsorption capacity (mg/g)	Reference
Iron oxide nanoparticles	36.0 (0.17 mmol/g)	This study
Humic acid	22.7	[11]
Goethite	11.04	[11]
Al_2O_3-supported iron oxide	28.98	[37]
Sand	0	[41]
Iron-coated sand	1.21	[42]
Manganese oxide-coated sand	1.34	[43]
Montmorillonite	33	[44]
Al_2O_3	17.5	[45]
Diatomite	24	[46]
Manganese oxide–carbon nanotube	26.24	[47]
Sawdust	3.19	[48]
Activated carbon (Merck)	21.5	[49]
Carbon nanotubes	17.44	[50]

3.7. Thermodynamic studies

Effect of temperature on the adsorption process provides valuable information not only on the type of process but also it provides knowledge about standard Gibbs free energy (ΔG^o_{ads}), standard enthalpy (ΔH^o_{ads}) and standard entropy (ΔS^o_{ads}) changes during the adsorption. ΔG^o_{ads} can be determined using the Langmuir constant, K_L, by the following equation [54]:

$$\Delta G^o_{ads} = -RT \ln K \quad (8)$$

where R is the ideal gas constant ($R = 8.314$ J/mol K), T is the temperature in Kelvin and K is the adsorption equilibrium constant

Table 2
Estimated parameters for the Langmuir and Freundlich models at different temperatures and pH = 5.5.

Temperature (K)	Freundlich constants			Langmuir constants		
	K_F (mmol/g) (L/mmol)$^{1/n}$	$1/n$ (unitless)	χ^2	K_L (L/mmol)	Q_m (mmol/g)	χ^2
298	0.128	0.076	0.001	24.6	0.14	0.001
313	0.145	0.074	0.001	28.6	0.15	0.01
328	0.167	0.070	0.001	33.1	0.17	0.1

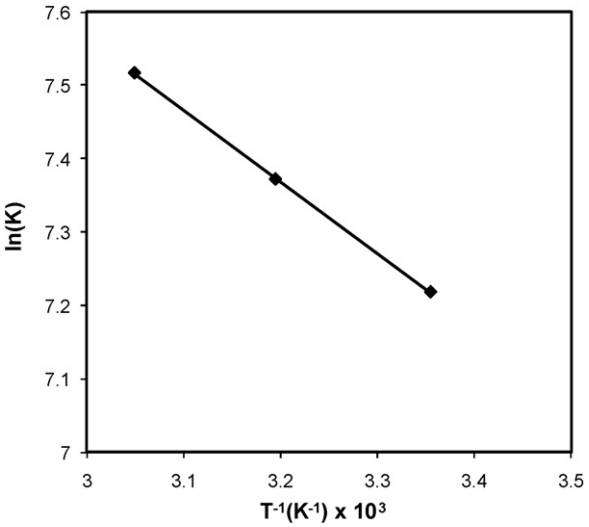

Fig. 7. Determination of thermodynamic parameters for the adsorption of Pb(II) onto Fe_3O_4 nanoadsorbents.

(dimensionless). K can be expressed as $K_L \times C_s$, where K_L is the equilibrium Langmuir constant (L/mmol) and C_s is the solvent molar concentration (mM), which can be calculated from the density and molecular weight of water at the given temperature. ΔH^o_{ads} and ΔS^o_{ads} can be determined from van't Hoff equation [54] that showed the dependence of equilibrium constant of the adsorption process on temperature as follows:

$$\ln K = -\frac{\Delta H^o_{ads}}{RT} + \frac{\Delta S^o_{ads}}{R} \quad (9)$$

The van't Hoff plot is presented in Fig. 7. The plot of ln(K) versus $1/T$ was found to be linear with a correlation coefficient $R^2 = 1.0$. ΔH^o_{ads} and ΔS^o_{ads} were calculated from the slope and intercept, respectively. The thermodynamic parameters at the studied temperatures are listed in Table 4. As seen, ΔG^o_{ads} at all temperatures was a negative value, confirming the spontaneous nature and the thermodynamically favorable adsorption. The further increase in the negative value of ΔG^o_{ads} the stronger the driving force of adsorption process. The positive value of ΔH^o_{ads} implies that the interaction between Pb(II) ions and nanoadsorbents is endothermic in nature, while the positive value of ΔS^o_{ads} may be attributed to the increase in randomness at the solid–liquid interface. This increase results from the extra translational entropy gained by the water molecules previously adsorbed onto nanoadsorbents but displaced by Pb(II) ions. It is noteworthy that adsorption process with ΔG^o_{ads} values between −20 and 0 kJ/mol corresponds to spontaneous physical process, while that with values between −80 and −400 kJ/mol corresponds to chemisorptions [55,56]. From the ΔG^o_{ads} values obtained in this study, it can be deduced that the adsorption mechanism is dominated by physisorption. This also is supported by the fact that $\Delta H^o_{ads} < 40$ kJ mol, indicating physical adsorption process [55].

Table 4
Estimated values of ΔG^o_{ads}, ΔH^o_{ads}, ΔS^o_{ads} for the adsorption of Pb(II) ions onto Fe_3O_4 nanoadsorbents at different temperatures.

Temperature (K)	$-\Delta G^o_{ads}$ (kJ/mol)	ΔH^o_{ads} (kJ/mol)	ΔS^o_{ads} (J/mol K)	R^2
298	17.9	8.1	87.1	1.0
313	19.2			
328	20.0			

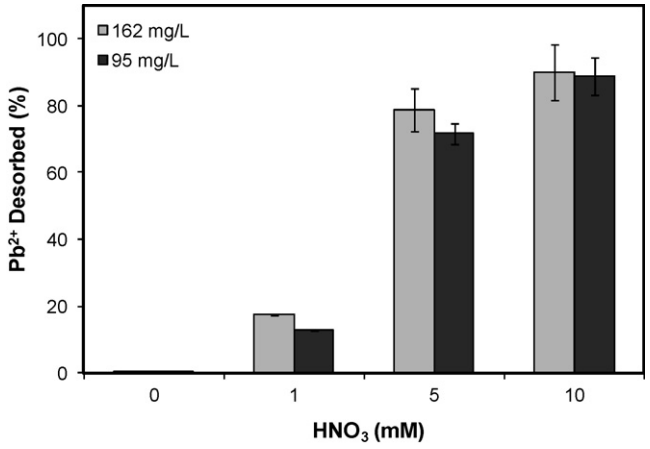

Fig. 8. Desorption of Pb(II) from Pb(II)-loaded Fe_3O_4 nanoadsorbents using different concentration of HNO_3 solution at fixed initial concentration of Pb(II): 95 and 162 mg/L, adsorbent dose: 10 g/L, shaking rate: 200 rpm, contact time: 2 h, T = 298 K.

3.8. Desorption of Pb(II)

Desorption of Pb(II) has two advantages, namely valuable Pb(II) ions can be recovered and nanoadsorbents can be re-used for another cycle. From the pH study, it has been found that adsorption of Pb(II) ions is highly dependent on pH. Therefore, the desorption of Pb(II) can be achieved by decreasing the pH of solution. Fig. 8 shows that the desorption efficiency increased with the increase in HNO_3 concentration. Insignificant desorption was achieved without additional HNO_3; while almost 90% recovery was obtained at 10 mM HNO_3, independent of the adsorbed Pb(II) concentration. This suggests that the adsorption of Pb(II) onto Fe_3O_4 nanoadsorbents is reversible, and the bonding between the active sites and the adsorbed Pb(II) is not strong. The results also suggest that the Pb(II)-loaded nanoadsorbents can be easily desorbed using a very low concentration of acid, and Fe_3O_4 nanoadsorbents has the potential to be used as an adsorbent for the removal and recovery of metal ions from wastewater. It is worth noting that, no obvious Fe ions were observed in the solution with the change in pH as detected by the ICP. This indicates that the dissolution of Fe_3O_4 nanoadsorbents during the desorption process was not an issue.

3.9. Reusability of nanoadsorbents

Fig. 9 shows the removal efficiency, R(%), of Pb(II), during a five cycles of adsorption–desorption–regeneration, from a 10-mL solution of initial Pb(II) concentration 162 mg/L at pH 5.5. As seen, no significant decrease in the adsorption capacity of Fe_3O_4 nanoadsorbents during the five cycles was observed. The results demonstrated that Fe_3O_4 nanoadsorbents can be used for the removal and recovery of metal ions from wastewater over a number of cycles, indicating its suitability for the design of a continuous process.

It is noteworthy that commercially available adsorbents such as, activated carbons are costly, time-consuming and its regeneration is essential. Actually, the regeneration and recovery of spent activated carbons is the most expensive part of the adsorption technology and it accounts for about 75% of the total operating and maintenance costs [34]. However, it seems this is not the case for the regeneration of spent Fe_3O_4 nanoadsorbents. Therefore, Fe_3O_4 nanoadsorbent is a cost-effective alternative with fast adsorption rate and its regeneration is simple and may be not necessary, especially for *in situ* application.

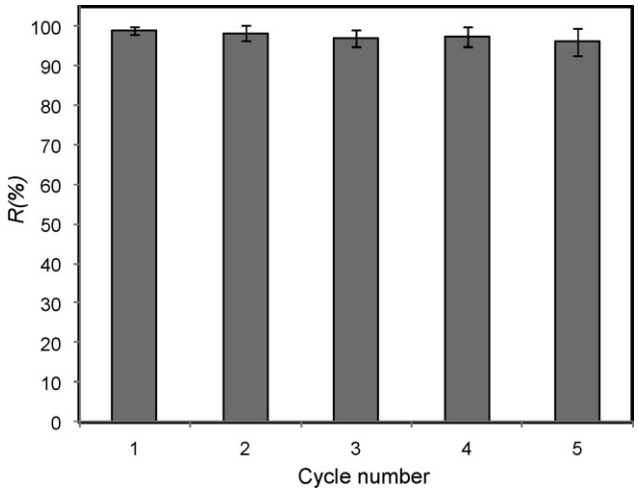

Fig. 9. Reusability of Fe_3O_4 nanoadsorbents for adsorption/desorption of Pb(II) during five cycles. Adsorption: initial concentration of Pb(II): 162 mg/L, adsorbent dose: 10 g/L, shaking rate: 200 rpm, contact time: 2 h, T = 298 K. Desorption: pH values between 2 and 3.

4. Conclusions

This study showed that Fe_3O_4 nanoadsorbents could be used as an alternate to conventional adsorbents for the removal of metal ions from wastewater in a very short time with high removal efficiency. The removal of Pb(II), as a typical metal ion commonly present in wastewater, by adsorption onto Fe_3O_4 nanoadsorbents was successfully accomplished. Adsorption was very rapid and equilibrium was achieved in less than 30 min. Also adsorption was highly dependent on the initial concentration of Pb(II), pH and temperature. Maximum removal was observed at pH 5.5. Adsorption increased as the initial concentration of Pb(II) and temperature increased. The adsorption isotherms were also determined and were appropriately described by both Langmuir and Freundlich models, with a better fitting to the Freundlich model than the Langmuir model. The thermodynamics of Pb(II) adsorption onto the Fe_3O_4 nanoadsorbents confirmed the endothermic nature of the adsorption process, the spontaneity and the physisorption of the process. The desorption and regeneration studies indicated that nanoadsorbents can be used repeatedly, without impacting the adsorption capacity. Therefore, Fe_3O_4 nanoadsorbents are recommended as fast, effective and inexpensive adsorbents for rapid removal and recovery of metal ions from wastewater effluents.

Acknowledgment

The author thanks Mr. Aashish Ragani and Ms. Keran Masoud for their technical help in the experimental work.

References

[1] J.R. Anderson, C.O. Weiss, Method for precipitation of heavy metal sulphides, USA, Patent, 3740331 (June, 19 1973).
[2] A. Smara, R. Delimi, E. Chainet, J. Sandeaux, Removal of heavy metals from diluted mixtures by a hybrid ion-exchange/electrodialysis process, Sep. Purif. Technol. 57 (2007) 103–110.
[3] I. Metcalf, Eddy, Wastewater Engineering Treatment and Reuse, 4th ed., McGraw Hill, New York, 2003.
[4] W.R. Peters, E.T. White, Y.K. Carole, S. Shedroll, Wastewater treatment–physical and chemical methods, J. Water Pollut. Control Fed. 58 (1986) 481–489.
[5] J. Patterson, Industrial Wastewater Treatment Technology, 2nd ed., Butterworth Publisher, Boston, 1985.
[6] J. Esalah, M.M. Husein, Removal of heavy metals from aqueous solutions by precipitation–filtration using novel organo-phosphorus ligands, Sep. Sci. Technol. 43 (2008) 3461–3475.
[7] B.A. Winfield, The treatment of sewage effluents by reverse osmosis—pH based studies of the fouling layer and its removal, Water Res. 13 (1979) 561–564.
[8] S.R. Shukla, S.P. Roshan, Removal of Pb(II) from solution using cellulose-containing materials, J. Chem. Technol. Biotechnol. 80 (2005) 176–183.
[9] G. Yan, T. Viraraghavan, Heavy-metal removal from aqueous solution by fungus Mucor rouxii, Water Res. 37 (2003) 4486–4496.
[10] R. Shawabkeh, A. Al-Harahsheh, M. Hami, A. Khlaifat, Conversion of oil shale ash into zeolite for cadmium and lead removal from wastewater, Fuel 83 (2004) 981–985.
[11] Z. Wu, Z. Gu, X. Wang, L. Evans, H. Guo, Effects of organic acids on adsorption of lead onto montmorillonite, goethite and humic acid, Environ. Pollut. 121 (2003) 469–475.
[12] M. Nasiruddin Khan, M. Farooq Wahab, Characterization of chemically modified corncobs and its application in the removal of metal ions from aqueous solution, J. Hazard. Mater. 141 (2007) 237–244.
[13] M. Kobya, E. Demirbas, E. Senturk, M. Ince, Adsorption of heavy metal ions from aqueous solutions by activated carbon prepared from apricot stone, Bioresour. Technol. 96 (2005) 1518–1521.
[14] B.S. Inbaraj, N. Sulochana, Carbonised jackfruit peel as an adsorbent for the removal of Cd(II) from aqueous solution, Bioresour. Technol. 94 (2004) 49–52.
[15] J. Hu, G. Chen, I.M.C. Lo, Removal and recovery of Cr(VI) from wastewater by maghemite nanoparticles, Water Res. 39 (2005) 4528–4536.
[16] R.Q. Long, R.T. Yang, Carbon nanotubes as superior sorbent for dioxin removal, J. Am. Chem. Soc. 123 (2001) 2058–2059.
[17] P.G. Tratnyek, R.L. Johnson, Nanotechnologies for environmental cleanup, Nano Today 1 (2006) 44–48.
[18] Y.C. Sharma, V. Srivastava, S.N. Upadhyay, C.H. Weng, Alumina nanoparticles for the removal of Ni(II) from aqueous solutions, Ind. Eng. Chem. Res. 47 (2008) 8095–8100.
[19] Z. Ai, Y. Cheng, L. Zhang, J. Qiu, Efficient removal of Cr(VI) from aqueous solution with Fe@Fe_2O_3 Coreâ shell nanowires, Environ. Sci. Technol. 42 (2008) 6955–6960.
[20] K. Hristovski, A. Baumgardner, P. Westerhoff, Selecting metal oxide nanomaterials for arsenic removal in fixed bed columns: from nanopowders to aggregated nanoparticle media, J. Hazard. Mater. 147 (2007) 265–274.
[21] J. Hu, G. Lo, Chen, Fast removal and recovery of Cr(VI) using surface-modified jacobsite ($MnFe_2O_4$) nanoparticles, Langmuir 21 (2005) 11173–11179.
[22] J. Hu, I.M.C. Lo, G. Chen, Removal of Cr(VI) by magnetite nanoparticles, Water Sci. Technol. 50 (2004) 139–146.
[23] A. Uheida, M. Iglesias, C. Fontàs, M. Hidalgo, V. Salvadó, Y. Zhang, M. Muhammed, Sorption of palladium(II), rhodium(III), and platinum(IV) on Fe_3O_4 nanoparticles, J. Colloid Interface Sci. 301 (2006) 402–408.
[24] T.K. Naiya, A.K. Bhattacharya, S.K. Das, Adsorption of Pb(II) by sawdust and neem bark from aqueous solutions, Environ. Prog. 27 (2008) 313–328.
[25] C.F. Baes, R.E. Mesmer, The Hydrolysis of Cations, Wiley, New York, 1976.
[26] P. Roonasi, A. Holmgren, An ATR-FTIR study of sulphate sorption on magnetite; rate of adsorption, surface speciation, and effect of calcium ions, J. Colloid Interface Sci. 333 (2009) 27–32.
[27] S.B. Johnson, G.V. Franks, P.J. Scales, D.V. Boger, T.W. Healy, Surface chemistry–rheology relationships in concentrated mineral suspensions, Int. J. Miner. Process. 58 (2000) 267–304.
[28] A. Uheida, G. Salazar-Alvarez, E. Björkman, Z. Yu, M. Muhammed, Fe_3O_4 and g-Fe_2O_3 nanoparticles for the adsorption of Co^{2+} from aqueous solution, J. Colloid Interface Sci. 298 (2006) 501–507.
[29] H. Sun, X. Zhang, Q. Niu, Y. Chen, J. Crittenden, Enhanced accumulation of arsenate in carp in the presence of titanium dioxide nanoparticles, Water Air Soil Pollut. 178 (2007) 245–254.
[30] P.K. Dutta, A.K. Ray, V.K. Sharma, F.J. Millero, Adsorption of arsenate and arsenite on titanium dioxide suspensions, J. Colloid Interface Sci. 278 (2004) 270–275.
[31] S.-Z. Lee, L. Chang, H.-H. Yang, C.-M. Chen, M.-C. Liu, Adsorption characteristics of lead onto soils, J. Hazard. Mater. 63 (1998) 37–49.
[32] L. Lv, M.P. Hor, F. Su, X.S. Zhao, Competitive adsorption of Pb^{2+}, Cu^{2+}, and Cd^{2+} ions on microporous titanosilicate ETS-10, J. Colloid Interface Sci. 287 (2005) 178–184.
[33] M.M. Benjamin, J.O. Leckie, Multiple-site adsorption of Cd, Cu, Zn, and Pb on amorphous iron oxyhydroxide, J. Colloid Interface Sci. 79 (1981) 209–221.
[34] V.J. Inglezakis, S.G. Poulopoulos, Adsorption, Ion Exchange and Catalysis: Design of Operations and Environmental Applications, Elsevier, UK, 2006.
[35] D.P. Rodda, B.B. Johnson, J.D. Wells, Modeling the effect of temperature on adsorption of lead(II) and zinc(II) onto goethite at constant pH, J. Colloid Interface Sci. 184 (1996) 365–377.
[36] E. Eren, Removal of lead ions by Unye (Turkey) bentonite in iron and magnesium oxide-coated forms, J. Hazard. Mater. 165 (2009) 63–70.
[37] Y.-H. Huang, C.-L. Hsueh, C.-P. Huang, L.-C. Su, C.-Y. Chen, Adsorption thermodynamic and kinetic studies of Pb(II) removal from water onto a versatile Al_2O_3-supported iron oxide, Sep. Purif. Technol. 55 (2007) 23–29.
[38] I. Langmuir, The constitution and fundamental properties of solids and liquids. Part I. Solids, J. Am. Chem. Soc. 38 (1916) 2221–2295.
[39] H.M.F. Freundlich, Uber die adsorption in losungen, Z. Phys. Chem. 57 (A) (1906) 385–470.
[40] D.C. Montgomery, G.C. Runger, Applied Statistics and Probability for Engineers, 4 ed., John Wiley & Sons, New York, 2006.
[41] A. Kaya, S. Durukan, Utilization of bentonite-embedded zeolite as clay liner, Appl. Clay Sci. 25 (2004) 83–91.
[42] C.H. Lai, C.Y. Chen, Removal of metal ions and humic acid from water by iron-coated filter media, Chemosphere 44 (2001) 1177–1184.

[43] R. Han, Z. Lu, W. Zou, W. Daotong, J. Shi, Y. Jiujun, Removal of copper(II) and lead(II) from aqueous solution by manganese oxide coated sand: II. Equilibrium study and competitive adsorption, J. Hazard. Mater. 137 (2006) 480–488.
[44] K.G. Bhattacharyya, S.S. Gupta, Adsorptive accumulation of Cd(II), Co(II), Cu(II), Pb(II), and Ni(II) from water on montmorillonite: influence of acid activation, J. Colloid Interface Sci. 310 (2007) 411–424.
[45] J. Yin, Z. Jiang, G. Chang, B. Hu, Simultaneous on-line preconcentration and determination of trace metals in environmental samples by flow injection combined with inductively coupled plasma mass spectrometry using a nanometer-sized alumina packed micro-column, Anal. Chim. Acta 540 (2005) 333–339.
[46] Y. Al-Degs, M.A.M. Khraisheh, M.F. Tutunji, Sorption of lead ions on diatomite and manganese oxides modified diatomite, Water Res. 35 (2001) 3724–3728.
[47] S.-G. Wang, W.-X. Gong, X.-W. Liu, Y.-W. Yao, B.-Y. Gao, Q.-Y. Yue, Removal of lead(II) from aqueous solution by adsorption onto manganese oxide-coated carbon nanotubes, Sep. Purif. Technol. 58 (2007) 17–23.
[48] B. Yu, Y. Zhang, A. Shukla, S.S. Shukla, K.L. Dorris, The removal of heavy metals from aqueous solutions by sawdust adsorption—removal of lead and comparison of its adsorption with copper, J. Hazard. Mater. 84 (2001) 83–94.
[49] J. Rivera-Utrilla, I. Bautista-Toledo, M.A. Ferro-García, C. Moreno-Castilla, Activated carbon surface modifications by adsorption of bacteria and their effect on aqueous lead adsorption, J. Chem. Technol. Biotechnol. 76 (2001) 1209–1215.
[50] Y.-H. Li, S. Wang, J. Wei, X. Zhang, C. Xu, Z. Luan, D. Wu, B. Wei, Lead adsorption on carbon nanotubes, Chem. Phys. Lett. 357 (2002) 263–266.
[51] T.K. Naiya, A.K. Bhattacharya, S.K. Das, Adsorption of Cd(II) and Pb(II) from aqueous solutions on activated alumina, J. Colloid Interface Sci. 333 (2009) 14–26.
[52] T.K. Naiya, A.K. Bhattacharya, S.K. Das, Clarified sludge (basic oxygen furnace sludge) – an adsorbent for removal of Pb(II) from aqueous solutions – kinetics, thermodynamics and desorption studies, J. Hazard. Mater. 170 (2009) 252–262.
[53] T.K. Naiya, A.K. Bhattacharya, S. Mandal, S.K. Das, The sorption of lead(II) ions on rice husk ash, J. Hazard. Mater. 163 (2009) 1254–1264.
[54] J.M. Smith, H.C. VanNess, M.M. Abbott, Introduction to Chemical Engineering Thermodynamics, McGraw Hill, New York, 2005.
[55] Y. Seki, K. Yurdakoç, Adsorption of promethazine hydrochloride with KSF montmorillonite, Adsorption 12 (2006) 89–100.
[56] Y. Yu, Y.-Y. Zhuang, Z.-H. Wang, Adsorption of water-soluble dye onto functionalized resin, J. Colloid Interface Sci. 242 (2001) 288–293.